NUMERICAL INVESTIGATION OF THE INFLUENCE OF BLADE SKEW AND GAP GEOMETRY ON SOUND RADIATION OF AXIAL VEHICLE COOLING FANS

Marcus BECHER, Florian ZENGER, Matthias TAUTZ,
Christoph SCHEIT, Stefan BECKER

Friedrich-Alexander University of Erlangen-Nuremberg,
Institute of Process Machinery and Systems Engineering,
Fluid System Dynamics and Aeroacoustics,
Cauerstrasse 4, 91058 Erlangen, Germany

SUMMARY

This paper focuses on the numerical calculation of sound generation and radiation caused by axial vehicle cooling fans. To investigate the influence of sound radiation dependent on gap geometry and blade skew, three fans with different geometries are taken into account. In terms of numerical simulation, a hybrid approach is chosen where first a CFD simulation is performed and the sound radiation is calculated in a second step. For the acoustic simulation an integral method described by Ffowcs-Williams-Hawkings is used to calculate the sound propagation into the far-field. These acoustical results are validated with experiments.

INTRODUCTION

The overall acoustic impression is an important factor in the decision of a customer to purchase a particular vehicle. This is one of the reasons why the automotive industry and its suppliers are interested in the sound design and acoustical optimization of vehicles and their components. A second driving force is the increasingly stringent legislation concerning vehicular sound emission which was implemented against the background of noise pollution in major population centers.

To optimize vehicles, specific components and systems which are responsible for noise generation are considered individually. One dominant noise source and central part of the engine cooling is the axial cooling fan.

Figure 1: Overall engine cooling system in vehicles

In the aerodynamic design of fans, CFD programs have been used successfully for years in terms of optimization and the prediction of fluid mechanical efficiency. For the acoustic design and the prediction of sound, numerical simulations have only seen limited use so far.

PEROT [1] uses the Lattice Boltzmann method and calculates flow and acoustics at the same time to predict sound radiation while MOREAU [2] chooses an approach for noise prediction which is based on the separation of tonal and broadband noise. In the present numerical investigations, a hybrid approach is chosen where first a CFD simulation based on the Navier-Stokes-Equations, using an SAS-turbulence-model, is performed and the acoustic is calculated in a second step. An integral method described by Ffowcs-Williams-Hawkings (FW-H) is used for the acoustic simulation.

ZAYANI [3] carries out experimental investigations of the hydrodynamic and acoustic behaviour of differently skewed axial automotive fans and explains its different efficiencies numerically, using stationary simulation results. The focus in this paper is on the influence of blade skew and geometrical modification of the gap geometry between the impeller and the housing on the radiation of sound. Three fans are investigated. A backward skewed fan with a standard gap geometry, the same fan with a modified gap geometry and a forward skewed fan with the standard gap geometry are taken into account.

The simulation results are validated with experiments. The corresponding setup in experiments and simulation represents an overall system which includes the cooler, the cooling fan and a combustion engine dummy.

EXPERIMENTAL SETUP

A DIN EN ISO 5801 normalized test bench exists at the Institute of Process Machinery and Systems Engineering. The test chamber was built to measure fluid mechanical behavior at various inflow and outflow conditions and the resulting acoustical performance of axial flow fans due to different installation conditions in an overall system. To reproduce the setup existing in the vehicle, the cooler, the axial cooling fan and a combustion engine dummy are part of the measurements.

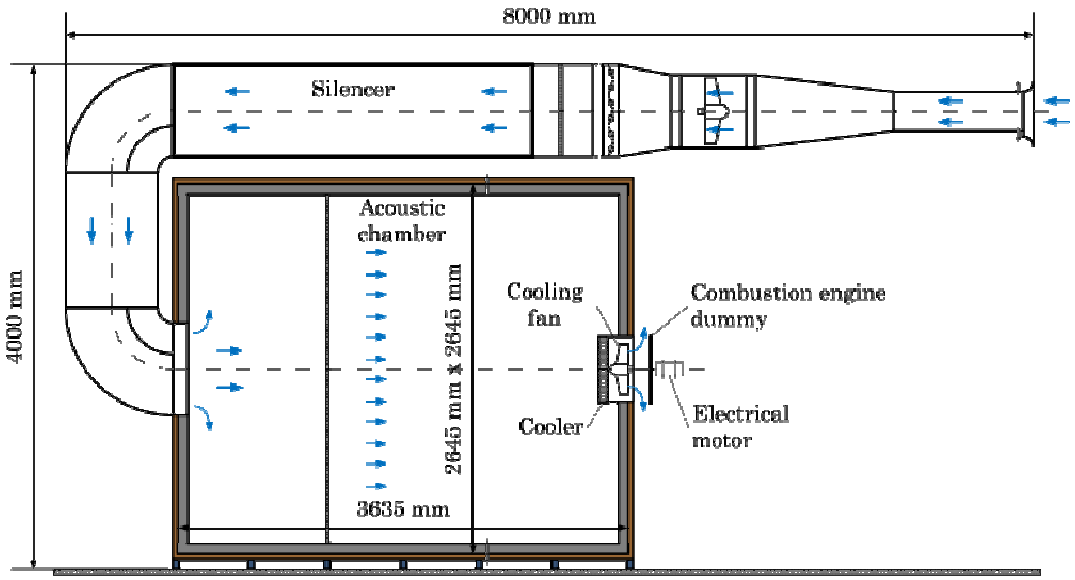

Figure 2: DIN EN ISO 5801 standardized test chamber including an acoustic chamber

The nine-blade axial cooling fans investigated in this paper are illustrated in figure 3. The first cooling fan is backward skewed and is driven with a standard gap (CF_BWS_SG). The second fan has the same blade shape as the first fan but is different in regards of the gap geometry (CF_BWS_MG). The third fan which is investigated is forward skewed and runs with the standard gap (CF_FWS_SG). The diameter of all three fans to the blade tips is 466 mm and the complete diameter which also contains a ring connecting the blades is 492 mm with the standard gap and 488mm in case of the modified gap configuration. The radial gap between the ring and the housing is about 7 mm in axial and about 6mm in radial direction.

Figure 3: Investigated axial cooling fans with different gap geometries

The cooling fan has to produce the fluid mechanical energy which is necessary for the air to flow through the cooler, positioned in front of the fan. Thus, the fan is designed to compensate at least the fluid-mechanical resistance to reach the desired cooling efficiency. Consequently, the pressure gradient over the cooler and fan has to be equal to zero. At the operating point, the cooling fans run

at a rotational speed of 2400 rpm and generate volumetric airflows of 1.1 m^3/s (CF_BWS_SG), 1.2 m^3/s (CF_BWS_MG) and 1.0 m^3/s (CF_VWS_SG).

The measurement setup of the overall system contains the cooling fan, the cooler and a combustion engine dummy, but does not contain any struts or a stator to stabilize the electrical motor which is normally placed in the hub. Thus, the fan can not be driven by its originally motor. Instead, an external electric drive is used in the experimental setup which is positioned behind the combustion engine dummy to avoid the propagation of the motor sound into the acoustic chamber.

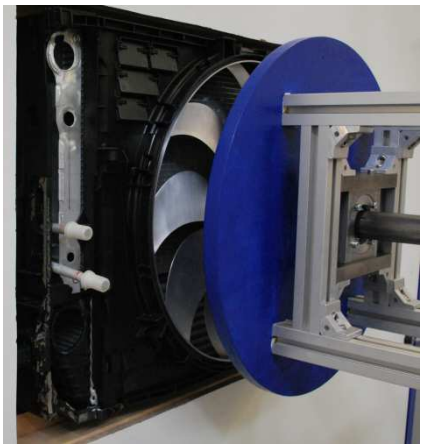

Figure 4: Experimental setup including cooler, fan and combustion engine dummy

The microphone is positioned at the suction side of the fan in the acoustic chamber, 1 m away from the cooler in the rotational axis of the fan. In the acoustic chamber, it is possible to have different far field conditions – a semi-free field, normally used for acoustical measurements and a full-free field according to the acoustic simulation.

NUMERICAL SETUP

Figure 5 shows a sectional view of the flow region, which is built up similar to the measurement setup, and consequently contains the cooler (c), the fan (f) and the dummy of the combustion engine (d).

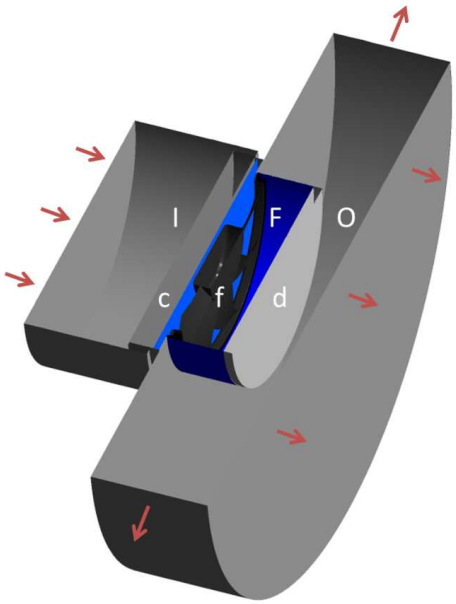

Figure 5: Sectional view of the simulated flow region splitted up in three subregions containing the cooler, the fan and the dummy of the combustion engine

The domain is divided into three subdomains, a stationary inlet area (I), the rotating domain with the fan (F) and a stationary outlet domain (O), connected by interfaces, colored blue in the previous figure. Due to the installation of cooler and combustion engine dummy, the flow through the simulated region has a main direction and does not contain any recirculation areas close to inlet and outlet surfaces. Thus, inlet and outlet region can be chosen relatively small compared to the dimensions of the fan. Important boundary conditions are free-field pressure conditions of 0 Pa at the inlet and outlet and the rotational speed of 2400 rpm for every configuration. No-slip conditions are used at surfaces which physically exist in the case of experiments like the fan and the combustion engine dummy. Slip conditions are chosen for surfaces which define the computational domain.

In the CFD simulation an SAS-turbulence-model [4] is applied, using a central difference spatial scheme and a second order backward Euler temporal scheme. This is a useful approach considering the challenges in the numerical calculation of sound. On the one hand, the turbulence model has to solve small scales which cause sound in high frequency ranges which leads to a small time increment and a high grid resolution. On the other hand, a long simulation time for predicting sound in low frequency ranges is needed which is possible due to the use of a relatively coarse grid, compared to Large-Eddy-Simulation.

The SAS-turbulence-model is an extended URANS-turbulence-model. It is also based on the distribution of the fluid mechanic variables of the Navier-Stokes-Equation in an averaged and a fluctuation value, but has an additional blending function to set down the turbulent viscosity locally, dependent on the grid size. Consequently, the grid resolution in areas where the main acoustic sources are produced has to be high enough to resolve the energy of small eddies, responsible for sound propagation at high frequency ranges.

The mesh resolution is mainly dictated by the need to resolve the boundary layer to consider the flow around the blades and the ring and its detachments which contribute to the propagation of sound on the one hand and the resolution of the further noise sources on the other hand. Taking account of these issues, the structured grid, including the whole computed domain, consists of about 45 Mio. nodes.

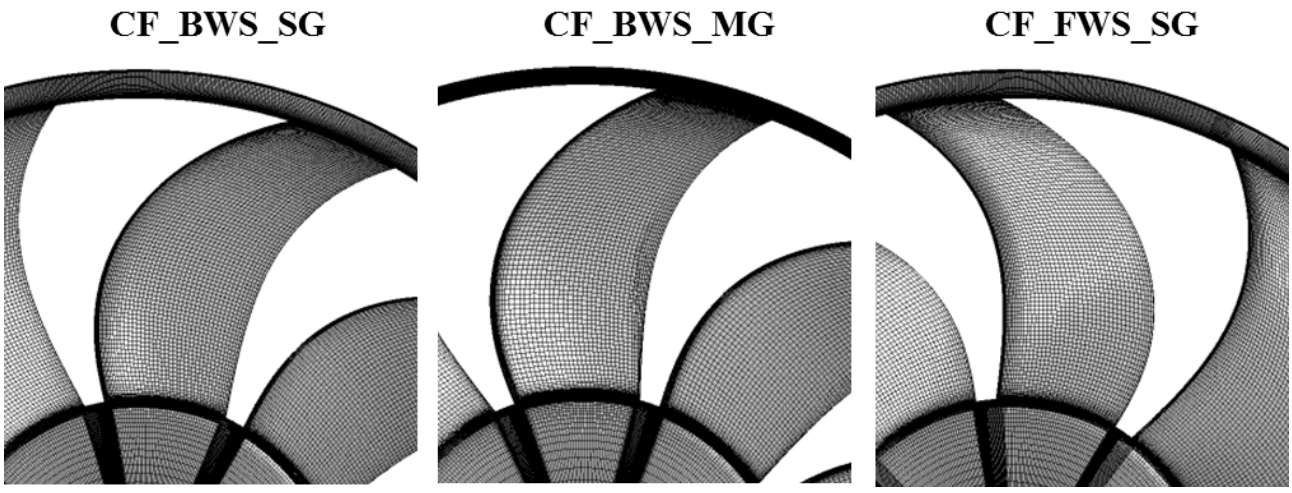

Figure 6: CFD-grid of the three fan configurations

On the one hand the time discretization is dictated by the CFL-number and on the other hand by the highest frequency which should be solved in the acoustic simulations. These criterions lead to a time step range Δt of $7 \cdot 10^{-6}$ s.

ACOUSTICAL METHODS

The code, used for the prediction of sound in this paper is called SPySI (sound prediction by surface integration) which is based on the Ffowcs Williams-Hawking method and was established by SCHEIT [5,6] and extended by HEINEMANN [7] at the Institute of Process Machinery and Systems Engineering. The calculation of acoustics is based on the following Ffowcs Williams-Hawkings equation:

$$4\pi\{p'H(f)\} = \frac{\partial^2}{\partial x_i \partial x_j}\int_{R^3}\left[\frac{T_{ij}H(f)}{r|M_r - 1|}\right]_{\tau_e} d^3\eta_j + \frac{\partial}{\partial t}\int_S\left[\frac{[\rho(u_i - v_i) + \rho_o v_i]n_i}{r|M_r - 1|}\right]_{\tau_e} dS(\eta_j) + \frac{\partial}{\partial x_j}\int_S\left[\frac{[\rho u_j(u_i - v_i) + P_{ij}]n_i}{r|M_r - 1|}\right]_{\tau_e} dS(\eta_j) \quad (1)$$

The first term of the equation at the right hand side includes the Heaviside function H(f), the radial Mach number M_r and the Lighthill stress tensor T_{ij} . It describes the quadrupol sources, in the case of a fan caused by the turbulence flow for example the turbulent wakes of the blades or eddy detachment at the ring which connects the blades.

The second term is named thickness noise and represents the source of sound which occurs due to the displacement of the air by a solid body, for example the blades of the fan. The size u_i corresponds to the fluid velocity and v_i characterizes the velocity of the surface.

The third and last term is called loading noise and describes the sound which is created by the moving force distribution on the air. In the example of a fan, it's caused by the time depending lift and drag forces acting on the passed air. This term also includes the compressive stress tensor P_{ij}.

$$P_{ij} = (p - p_0)\delta_{ij} + \tau_{ij} \quad (2)$$

For calculation of radiation of sound into the far-field to the microphone position, the FW-H equation can be solved with the free-space Green's function [8]:

$$G(x_i, y_i, t, \tau) = \frac{\delta(t - |x_i - y_i|/c_o - \tau)}{4\pi|x_i - y_i|} \quad (3)$$

In order to use SPySI for the FW-H calculation, the flow variables of interest - the velocity components, the pressure and the density - are interpolated to the permeable integration surface placed around the acoustic sources caused by the impeller and are exported from the CFD calculation at every third time step in this case. In these investigations the integration surface is placed between the cooler and the fan in the stationary domain. It should be positioned as close as possible to the acoustical sources to avoid the influence of numerical damping to the acoustical results but should only include acoustical pressure fluctuations. In the case of the whole fan, a slice is selected which covers the whole inlet area of the fluid region as plotted in figure 7.

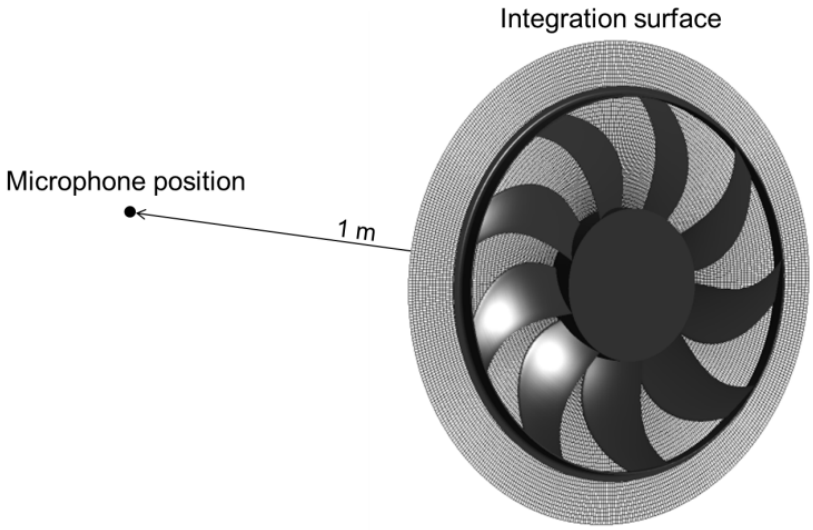

Figure 7: Acoustical simulation setup: Integration surface and microphone position

From this integration surface, Green's function is used to calculate the acoustically relevant parameters at a point that corresponds to the microphone position in experiments, 1 m on the rotational axis away from the cooler.

FLUID MECHANICAL RESULTS

In the following, the fluid mechanical results are presented with the main focus on the gap flow and its influence on the inflow conditions and sound generation. The gap flow is caused by the pressure gradient between the suction and the discharge side of the fan. The air flows through the gap from the discharge side to the suction side and interacts with the inflow. Turbulent structures are generated which impinge on the leading edge of the blades. In figure 8 these turbulent structures are illustrated by the isosurfaces of vorticity at 5000 s^{-1} which are colored by the velocity.

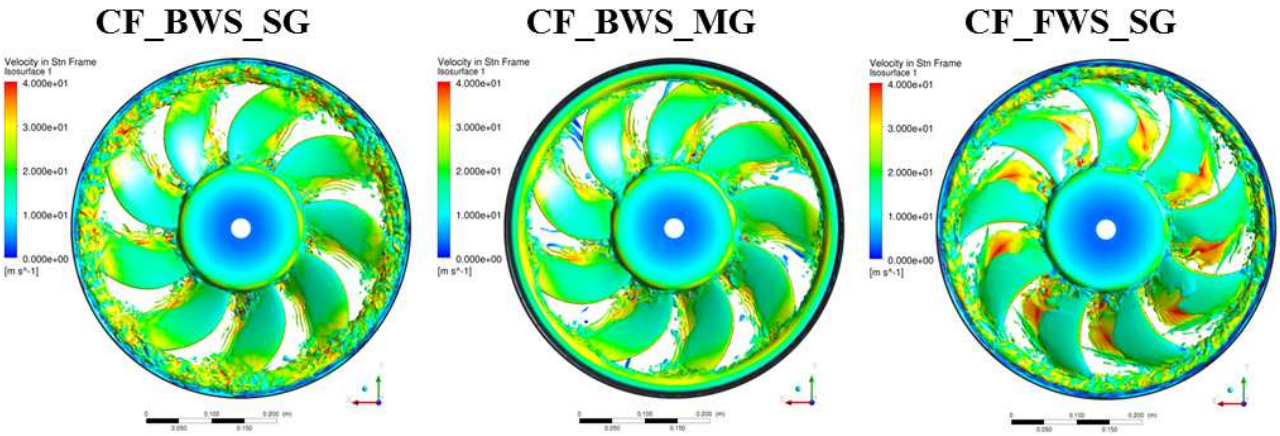

Figure 8: Turbulent structures of the three investigated fan configurations

To clarify the influence of different gap flows dependent on blade skew and gap geometry, streamlines are plotted on a sectional plane between the blades of the investigated fans.

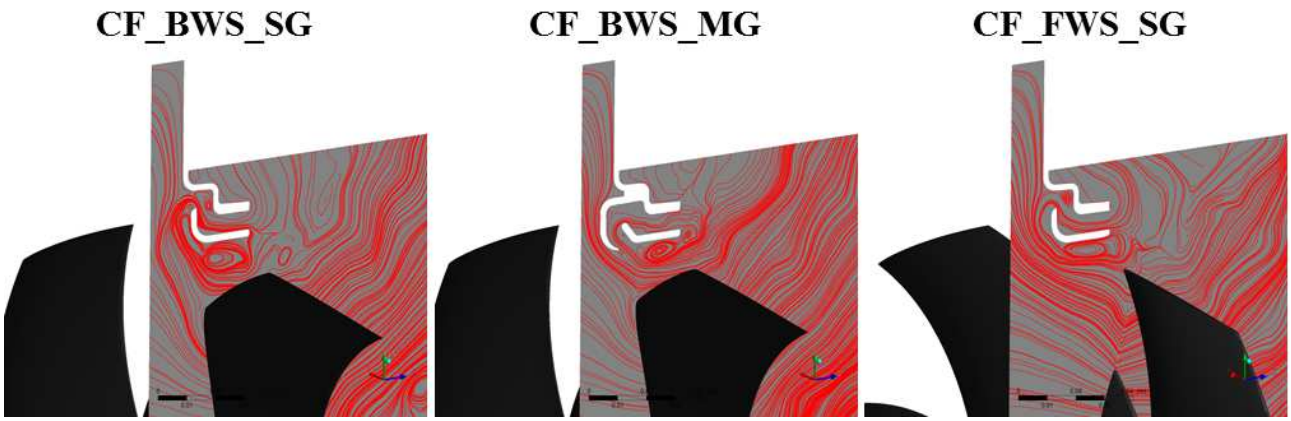

Figure 9: Streamlines on a sectional plane between the blades

The inflow and gap flow of the backward skewed fan with the standard gap geometry shows a dominant component of the velocity in the direction of the hub compared to the other configurations. This behavior can be explained by the shape of the blades. The gap flow between the blades follows the pressure gradient whose closest minimum is located at the suction side of the blades at about 4/5 of the radius of the blade (in the case of the backward skewed fan with the standard gap). In the configuration of the forward skewed fan the closest pressure minimum driving the gap flow is located at the tip of the blades which leads to a feeding of the gap flow to the tip and the dominant component of the inflow in the direction of the rotation axis. The modified gap geometry also minimizes a velocity component in the direction of the gap by supplying the gap flow to the tip of the blades.

As a result of the different gap flows at the suction side of the fan dependent on gap and blade geometry, a recirculation area arises beneath the ring which connects the tips of the blades. While gap modification and backward blade skew minimize its size, the combination of backward blade skew and standard gap leads to the deflection of the inflow and gap flow in the direction of the hub. This behavior supports the production of a large recirculation area between the blades which impinges on the leading edges of the blades and leads to different pressure fluctuations on the blades. To show this, in the following figure the RMS value of the fluctuation of the pressure is plotted on one of the blades.

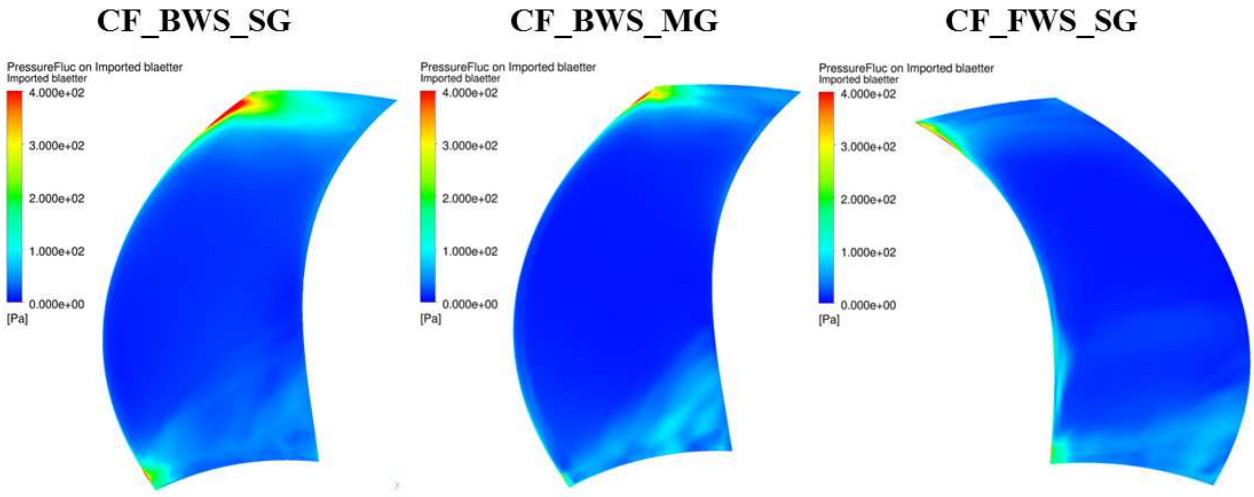

Figure 10: RMS value of pressure fluctuations, plotted on the surface of the blades

The influence of the size of the recirculation areas, dependent on the gap and blade geometry, on the RMS value of pressure is demonstrated in figure 10. At the leading edge and suction side of the blades at the area of the tip, the largest area with RMS values greater than 100 Pa can be detected in

case of the backward skewed fan with the standard geometry. With the gap modification, high pressure fluctuations can be reduced to a much smaller area. In case of the forward skewed fan, high pressure fluctuations mainly occur directly at the leading edge and not in that high pressure ranges compared to the backward skewed fans.

ACOUSTICAL RESULTS

In the following, the influence of the different flow conditions on the acoustical results is presented which contains the validation of the numerically calculated sound radiation with measurements in terms of sound propagation.

Figure 11 shows the comparison between measured and calculated sound radiation. The acoustical pressure of the three fan configurations is calculated with the in-house code SPySI at the microphone position that corresponds to the microphone position in experiments, 1 m on the rotational axis away from the cooler. In the following, the spectra of the measured and simulated time signal are compared. To obtain these, pwelch (window length of 0,05s, Hanning windowing) in Matlab is used in every case. The black simulated spectra are computed from the time signals with the length of 0.075 s which corresponds to three rotations of the fans. The spectra of the measurements are plotted in two ways. One time, the measurement signal of 10 s is plotted in dark red and additionally, this time signal is splitted up in time signals with the length of the simulation signal, plotted in light red, to reach a better comparability.

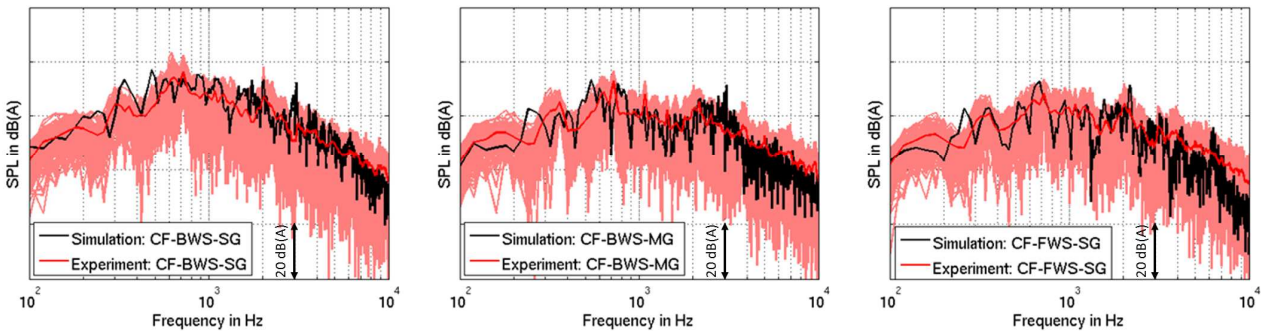

Figure 11: Calculated SPL spectra, validated with experiments

The acoustical computation indicates good to very good correlation with the measurements dependent on the frequency. In all three calculations, there is a very good match in the middle frequency range between 300 Hz and 3000 Hz. In the high frequency range, the simulated spectra of the backward skewed fan with the modified gap and the forward skewed fan underestimate the spectra of the averaged spectrum by a small margin. There are relative similar reasons. The configuration with the modified gap has the highest efficiency of the configurations which leads to a higher volume flow and a higher Reynolds number which requires a higher grid resolution. In the case of the forward skewed fan, a better grid resolution at the trailing edge is necessary to resolve smaller turbulent structures which are responsible for noise generation in the high frequency range. The low frequency range below 300 Hz fits well and can only be improved by increasing simulation time.

In Figure 12 experimental results and measured results are plotted separately to compare the influence of gap geometry and blade skew on the acoustic. To reach a better detection of the difference of the SPL in the different frequencies, third-octave-band spectra are used.

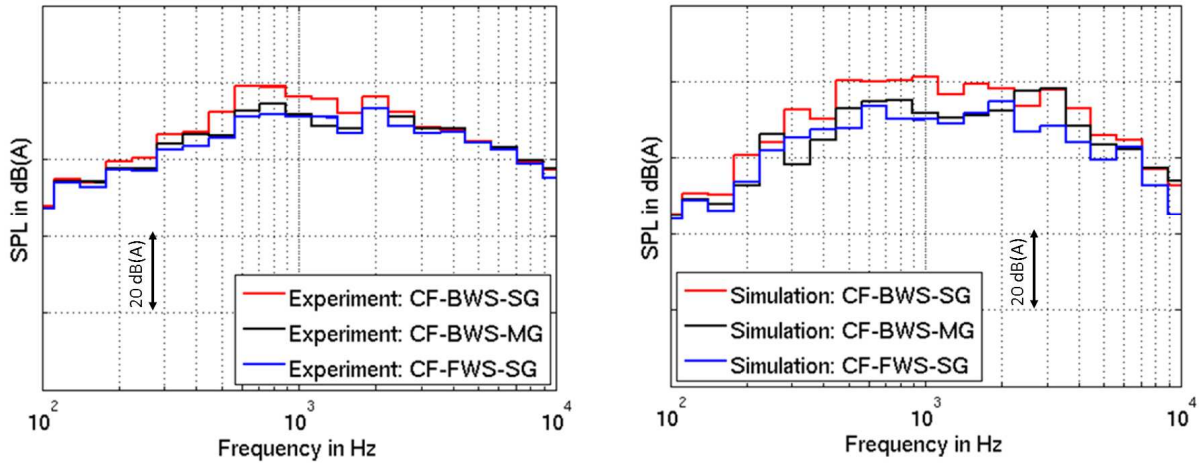

Figure 12: Calculated SPL spectra, validated with experiments

The experiment results show that there is a difference in the sound radiation of the fans. The cooling fan with the modified gap (black curve) and the configuration with the forward skewed blades (blue curve) reach about the same SPL in the considered frequency range. The fan with the standard geometry (red curve) has a higher sound radiation in the frequency range between 200 Hz and 3000 Hz of about 6 dB(A).

The higher SPL in this frequency range can be explained with the interaction of the surface of the blades with the already mentioned recirculation areas and turbulent gap flow, respectively, which leads to a much larger area of high pressure fluctuation in case of the fan with the backward skewed fan with the standard gap geometry, compared to the others. Thus, this effect is comparable with different turbulent inflow conditions which lead to an increase of the radiation of sound in a low frequency range dependent on the turbulent length of the eddies [9].

The simulation results in figure 12 show the same trends in the frequency range between 400 Hz and 2000 Hz. To reach better results in the low frequencies, a longer simulation time is necessary. A higher grid resolution and a different turbulence model could lead to better matching in the high frequency range.

CONCLUSION

The influence of blade skew and gap geometry on the flow field and the sound propagation was investigated for three fans with different geometries. A backward skewed fan with a standard gap geometry, the same fan with a modified gap geometry and a forward skewed fan with the standard gap geometry are taken into account. The fluid mechanical results show different gap flows at the suction side of the fan dependent on gap and blade geometry which leads to a production of different turbulent structures between the blades. In the cases of the backward skewed fan with the standard gap geometry a large recirculation area can be detected which impinges on the leading edge of the blades while the other configurations minimize the size of this recirculation area.

This behavior leads to a higher pressure fluctuation on the leading edge of the blades and thus, to a higher radiation of sound in the low frequency range in the case of the backward skewed fan with the standard gap geometry. This effect can be reproduced by the numerically calculated propagation of sound with the inhouse code SPySI based on the method of FW-H. In terms of sound prediction SPySI can become a useful tool to calculate the propagation of sound to a point in the far-field. The acoustical computation indicates good to very good agreement with the measurements depending on the frequency. Furthermore, measurements and simulation results show similar differences in the SPL at the middle frequency range.

BIBLIOGRAPHY

[1] Pérot, F. – *Direct Aeroacoustics Prediction of a Low Speed Axial Fan*, 16th AIAA/CEAS Aeroacoustics Conference, AIAA-2010-3887, **2010**

[2] Moreau, S. et al. – *Toward the prediction of low-speed fan noise*, Center for Turbulence Research, Proceedings of the Summer Program 2006, **2006**

[3] Zayani, M. et al – *Aeroacoustical investigations on axial fans for automotive cooling systems*, FAN 2012, **2012**

[4] Menter, F. – *Two-Equation Eddy-Viscosity Turbulence Models for Engineering Applications*, AIAA Journal, Vol.32(8), pp. 1598-1605, **1994**

[5] Scheit, C. – *Implementation of a Ffowcs Williams and Hawkings (FW-H) method for aeroacoustic prediction*, Master of Science thesis, University of Erlangen-Nuremberg, **2007**

[6] Scheit, C. et al – *Effect of blade wrap angle on efficiency and noise of small radial fan impellers – A computational and experimental study*, Journal of Sound and Vibration, No. 331, No. 5, pp. 996-1010, **2011**

[7] Heinemann, T. – *Implementation of a Ffowcs Williams and Hawkings (FW-H) formulation for moving surfaces*, Diploma thesis, University of Erlangen-Nuremberg, **2011**

[8] Ehrenfried, K. – *Strömungsakustik (Aeroacoustics),* Mensch & Buch Verlag, pp. 145-159, **2004**

[9] Zenger F. et al – *Influence of Inflow Turbulence on Aeroacoustic Noise of Low Speed Axial Fans with Skewed and Unskewed Blades*, FAN 2015, **2015**

NOMENCLATURE

c_0	velocity of sound	v_i	surface velocity
G(x,t)	Green's function	ρ	density
H(f)	Heaviside function	τ	retarded time
M_r	Radial Mach number	τ_{ij}	viscous forces
n_i	outward surface normal vector		
P_{ij}	Compressive stress tensor	FFT	Fast-Fourier-Transformation
r	Distance from source to observer	FW-H	Ffowcs Williams and Hawkings
t	time	SAS	Scale Adaptive Simulation
T_{ij}	Lighthill stress tensor	SPL	sound pressure level
u_i	fluid velocity	SPySI	Sound Propagation by Surface Integration